ISSN 0036-0244, Russian Journal of Physical Chemistry A, 2020, Vol. 94, No. 2, pp. 352–359. © Pleiades Publishing, Ltd., 2020.

STRUCTURE OF MATTER AND QUANTUM CHEMISTRY

Theoretical Study of the Substituent Effect on the Electronic Structure and Spectral Properties of Six Salicylaldehyde Schiff Bases

Luo Fei-Hua[a,b,*]

[a]*College of Materials Science and Engineering, Yangtze Normal University, Fuling, 408100 China*

[b]*College of Chemistry, Sichuan University, Chengdu, 610064 China*

**e-mail: 20180011@yznu.cn*

Received May 14, 2019; revised May 14, 2019; accepted July 9, 2019

Abstract—In the present work, the ground- and excited-state geometries for a series of salicylaldehyde hydrazones (SHs) were optimized including SH-Ph, Naph-SH-Ph, 3-OMe-SH-Ph, 4-NEt_2-SH-Ph, 3-F-SH-Ph, and 3-NO_2-SH-Ph at the PBE1PBE/6-31G(*d*,*p*) level, and the results agree well with the corresponding experimental data. By means of the TD-DFT method, the absorption and emission spectra were calculated based on the optimized ground-state and the excited-state geometries, respectively. It is found that the absorption and emission transition character can be altered by adjusting the electron-withdrawing and electron-donating groups or expanding the aromatic conjugation on salicylaldehyde. These results indicate that both absorption and emission properties are governed by the HOMO–LUMO gap (Δ_{H-L}) which is usually considered as the basis of the experimental design. In addition, the charge transport quality has been estimated approximately by the calculated reorganization energy (λ). The calculated results also show that the species of the substitute groups and the expanded aromatic ring affect the charge transfer rate and balance. All calculations reveal that introduction of strong electron-withdrawing or electron-donating substituents on the base of the expanded aromatic rings is expected to be a useful for the luminescent material design.

Keywords: salicylaldehyde hydrazone, fluorescent molecule, DFT calculation, HOMO–LUMO gap

DOI: 10.1134/S0036024420020235

INTRODUCTION

Fluorescence, which is spontaneous light emission coming from excited electronic states after absorption of UV/visible light, has received great attention in many disciplines, such as chemistry, physics, material science, medicine, and biology [1–4]. Salicylaldehyde Schiff bases were important typical fluorescent molecules, which were easy to synthesize and stable. It was also known to undergo excited-state intramolecular proton transfer process (ESIPT), which gives rise to large Stokes shifts and efficient emission [5, 6]. Several groups have demonstrated tuning of the fluorescence wavelength from blue and red, and the most common strategy is to adjust various electron-donating or electron-withdrawing substituents at different positions of the organic fluorescent molecules [7–10]. In 2015, Xiang et al. have reported the synthesis and the application of fluorescent pH probes of a series fluorescent Schiff bases containing different electron-withdrawing substituents (–NO_2, –F, and –Cl) and electron-donating substituents (–OMe and –NEt_2). The fluorescent molecules display strong blue, green, and red fluorescence as the substituents modified [11]. Recently, they also reported a series of simple and highly fluorescent salicylaldehyde hydrazone molecules with different substituents on the aromatic rings [12]. They found the molecules display strong blue, green, yellow, and orange aggregation-induced emission (AIE) with large Stokes shifts (up to 184 nm) and high fluorescence quantum yields (Φ up to 0.20) as the substituents varied.

On the other hand, computational chemistry has become an important tool for chemists and a well-accepted partner for experimental chemistry in these years. Theoretical quantum chemistry is an important area in determining the mechanisms of chemical reactions [13], structural determination of organic compounds [14], prediction of spectroscopic data such as UV/Vis and fluorescence properties of organic molecules [15, 16]. It is important to understand the relationship between structure and spectral property. In theory, the energy gap between the highest occupied molecular orbital (HOMO) and lowest unoccupied molecular orbital (LUMO) is often used to analyze the absorption and emission properties in theoretical design for this kind of materials. The theoretical studies (DFT calculations) were often used for interpreting the molecular structures, spectroscopic assignments [16, 17]. In this research, we inspired to used DFT calculations to investigate the ground- and excited-state geometries, HOMO–LUMO gaps, UV–Vis, fluores-

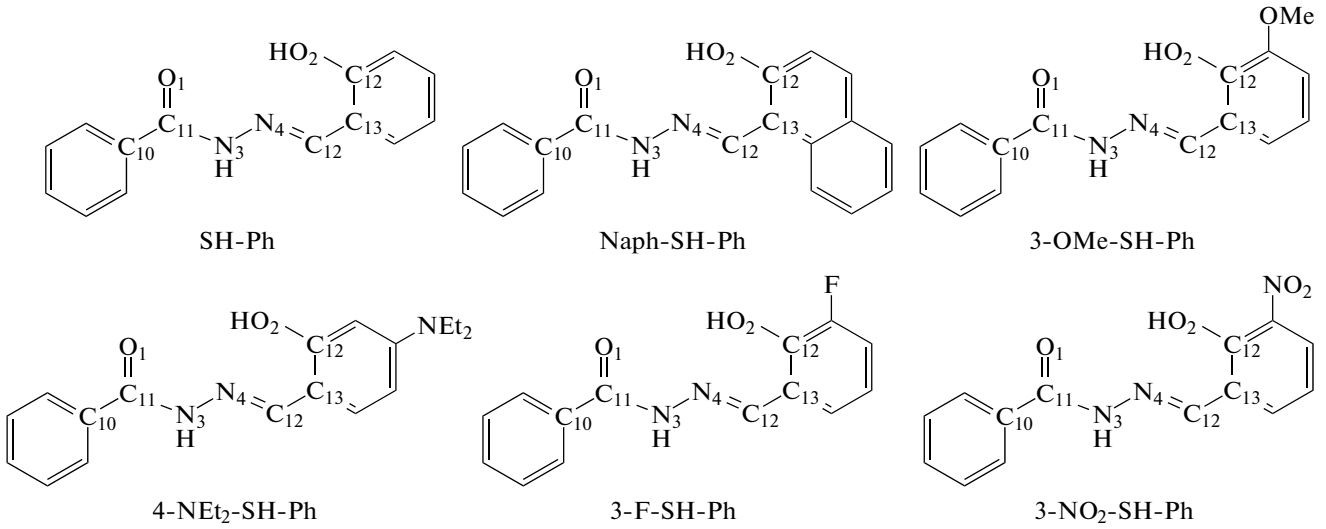

Fig. 1. The sketch map of the structures for the studied systems.

cence and reorganization energy (λ) of six reported salicylaldehyde hydrazones (SHs) containing different electron-withdrawing substituent (−F, $-NO_2$) and electron-donating substituents (−OMe, $-NEt_2$) at different position of the aromatic ring, and further explored the substituents effect on the electronic structure and spectral properties of the molecules.

COMPUTATIONAL METHODS

In this work, the quantum chemical calculations have performed and optimized six salicylaldehyde hydrazones (SHs) using the density functional theory (DFT) [18] method with 6-31g(*d*,*p*) basis sets by the Gaussian 09W program package [19] on a Pentium IV/3.60 GHz personal computer. The ground-state and the excited-state geometries were fully optimized by with PBE1PBE [20]. The Polarized Continuum Model (PCM) [15] was used for calculations. The absorption wavelengths (λ_{abs}) and emission wavelengths (λ_{em}) of these molecules in a solvent acetonitrile are systematically studied at the theoretical level of PBE1PBE/6-31g(*d*,*p*). The electronic properties such as E_{HOMO}, E_{LUMO}, energy gap between HOMO and LUMO and reorganization energy (λ) [21] of the title structures were calculated. The optimized molecular structures, HOMO and LUMO surfaces were visualized by GaussView05 program [22].

RESULTS AND DISCUSSION

Optimized Geometries

The schematics of the structures are depicted in Fig. 1, along with the optimized S_0 state geometries by PBE1PBE/6-31g(*d*,*p*) of the six salicylaldehyde hydrazones (SHs) plotted in Fig. 2. The important optimized structural parameters including bond lengths and dihedral angle of the molecules are listed in Table 1, and compared with the experimental data [12]. The calculated results are in agreement with the experimental values, the maximum deviation for bond lengths and dihedral angle are 0.0393 Å and 8.82°, respectively, indicating that the functional and basis set used are reasonable and feasible for the system under study.

The main difference between the studied compounds is that the π-conjugated system and the substitution of the salicylaldehyde are changed in the frameworks, compared to the molecule of SH-Ph. It was found that the substituent effect (SH-Ph, 3-OMe-SH-Ph, 4-NEt_2-SH-Ph, 3-F-SH-Ph, 3-NO_2-SH-Ph) on the salicylaldehyde may not cause significant changes in the optimized structures of the bonds and dihedral angle. But the dihedral angle of the two aromatic rings in the framework is reduced from 29.43° to 12.87° when the benzene ring is replaced by naphthalene (SH-Ph and Naph-SH-Ph). This indicated that the increasing π-conjugated aromatic rings of the system might increase the planarity of the molecule.

The optimized structures of S_1 states were also obtained using TD-DFT at PBE1PBE/6-31g(*d*,*p*) level. The dihedral angle between salicylaldehyde and benzoylhydrazine of the S_0 and S_1 state is depicted in Fig. 3. From Fig. 3, the dihedral angle differences between S_0 and S_1 states of four compounds (Naph-SH-Ph, 3-OMe-SH-Ph, 4-NEt_2-SH-Ph, 3-NO_2-SH-Ph) are below 15° except SH-Ph. Interestingly, the dihedral angle differences of compound 3-OMe-SH-Ph and 3-NO_2-SH-Ph are 0.13° and 2.68°, respectively which are much lower than other compounds. The tiny dihedral angle differences between S_0 and S_1 states indicate that the non-radiative decay

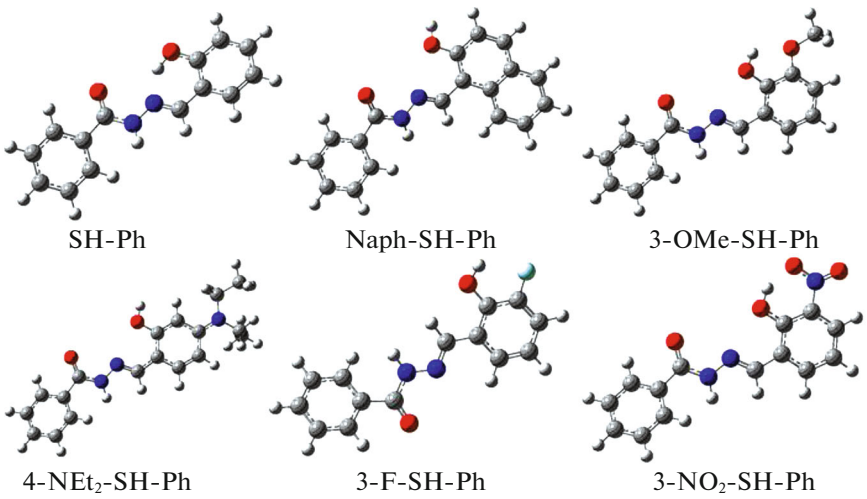

Fig. 2. (Color online) The stereograph of optimized structures of the SHs by PBE1PBE/6-31g(*d*,*p*).

from S_1 to S_0 is able to be suppressed effectively for the compounds [23].

The Frontier Molecular Orbitals Analysis

The influence of the electronic and luminescent properties is usually investigated by the molecular orbital analysis, especially excitation and transition properties can be reflected by the frontier molecular orbitals. The influence of a particular substituent on an aromatic system is usually investigated in terms of conjugated and induced effects, and the conjugated effect is usually associated with the sharing of π-electrons between the substituent and the aromatic system. The induced effect is related to the σ-electron system of the aromatic molecule. In general, the electron-withdrawing groups can make the energies of the highest occupied and lowest unoccupied MOs decreased, while the electron-donating groups cause an increase of the HOMOs and LUMOs energies.

The calculated HOMO and LUMO energies and electronic density contours are presented in Fig. 4. In contrast with SH-Ph, it is easy to see that HOMO and LUMO energies increase for the compound with electron-donating group on salicylaldehyde (3-OMe-SH-Ph, 4-NEt_2-SH-Ph) while for the electron-withdrawing groups the HOMO and LUMO energies decrease (3-F-SH-Ph, 3-NO_2-SH-Ph). The maximum difference of HOMOs energy is 0.84 eV appeared in 4-NEt_2-SH-Ph (HOMO: −5.35 eV) and that of LUMOs energy is 1.05 eV appeared in 3-NO_3-SH-Ph (LUMO: −2.68 eV). For 4-NEt_2-SH-Ph and 3-NO_3-SH-Ph, the HOMO–LUMO gaps (Δ_{H-L}) decrease 0.46 and 0.75 eV by comparing to SH-Ph, whereas they increase 0.02 eV for 3-OMe-SH-Ph and 0.11 eV for 3-F-SH-Ph. To explain these phenomena, select-

Table 1. Selected optimized important length (Å) and angle (deg) of SHs, as well as experimental data

Bond	SH-Ph	Exp.[a]	Naph-SH-Ph	3-OMe-SH-Ph	4-NEt_2-SH-Ph	3-F-SH-Ph	Exp.[a]	3-NO_2-SH-Ph
C10–C11	1.4912	1.5023	1.4948	1.4951	1.4966	1.4940	1.4884	1.4938
O1–C11	1.2233	1.2213	1.2233	1.2233	1.2255	1.2226	1.2283	1.2219
N3–C11	1.3726	1.3333	1.3699	1.3697	1.3651	1.3721	1.3473	1.3736
N3–N4	1.3479	1.3641	1.3539	1.3544	1.3601	1.3503	1.3693	1.3496
N4–C12	1.2868	1.2917	1.2848	1.2840	1.2875	1.2832	1.2733	1.2829
C12–C13	1.4489	1.4320	1.4584	1.4555	1.4468	1.4577	1.4474	1.4581
O2–C14	1.3397	1.3575	1.3473	1.3466	1.3497	1.3500	1.3444	1.3210
Angle[b]	29.43	24.02	12.87	32.94	28.9	31.9	40.72	34.59

[a]The experimental bonds and angle are from [12]. [b]The angle is the dihedral angle of aromatic rings between salicylaldehyde and benzoylhydrazine.

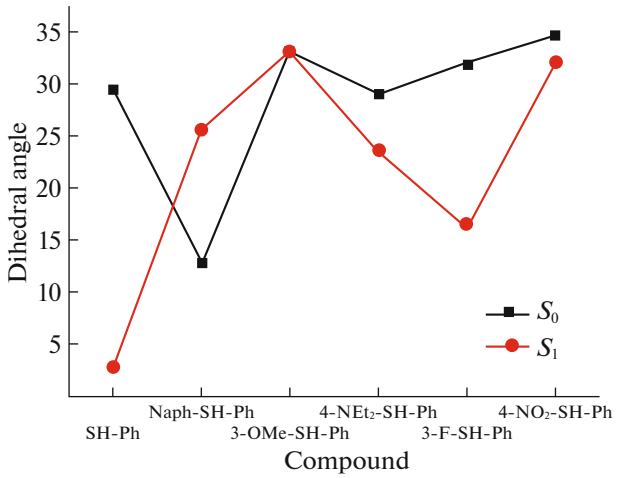

Fig. 3. (Color online) Dihedral angles of the six compounds at their S_0 and S_1 states.

ing frontier molecular orbitals of these complexes which are depicted in Fig. 4, for 4-NEt_2-SH-Ph, the HOMO is mostly localized on salicylaldehyde and imine while the LUMO is distributed throughout the framework, and the strong electron-donating group of NEt_2 could shared the *p* electron with salicylaldehyde by *p*–π conjugation, thus the strong *p*–π conjugated donation from the NEt_2 group raises the energy of HOMO level in evidence, resulting in the Δ_{H-L} decrease. For 3-NO_3-SH-Ph, the LUMO is focused on the phenyl part of salicylaldehyde, thus the electron-withdrawing substituent of nitro at the phenyl of salicylaldehyde will decrease the LUMO energies more than HOMO energies, resulting in the decreased Δ_{H-L}. Different from 3-NO_2-SH-Ph, the LUMO is distributed throughout the framework in the molecular 3-F-SH-Ph which will decrease the HOMO energies more than LUMO energies, so for 3-F-SH-Ph, the Δ_{H-L} is increased. In addition, the expansion of the conjugated salicylaldehyde for Naph-SH-Ph seems increase the HOMO energies and hence reduce the $\Delta_{H-L.}$ So the strong electron-donating (electron-withdrawing) substituents and extended conjugate system on salicylaldehyde can make evident decrease of the Δ_{H-L} for these molecules.

Absorption Spectra

Absorption spectra were calculated using TD-DFT method in acetonitrile solution on the base of optimized geometries. Table 2 reports the transition energies (*E*), oscillator strengths (*f*) and major configurations of the leading excited states with the largest amplitudes, along with their experimental values. As shown in Table 2, the S_1 absorption bands of compounds SH-Ph to 3-NO_2-SH-Ph are 322.83, 346.21, 319.53, 348.53, 309.86, and 403.12 nm, respectively. In addition, the excitation HOMO → LUMO (SH-Ph: 96.7%; Naph-SH-Ph: 97.8%; 3-OMe-SH-Ph: 95.3%; 4-NEt_2-SH-Ph: 98.5%; 3-F-SH-Ph: 95.5%; 3-NO_2-SH-Ph: 97.8%) are predominantly responsible for the absorption. Observing Fig. 4 concludes that the transitions of all electrons are typical π → π* types. All these results agree well with the variation tendency of Δ_{H-L}. Taking compound SH-Ph as a reference, the S_1 absorption peaks of compound 3-F-SH-Ph and 3-OMe-SH-Ph are blue-shifted, while others are red-shifted. In comparison with compound SH-Ph (322.83 nm), compounds 3-F-SH-Ph and 3-OMe-

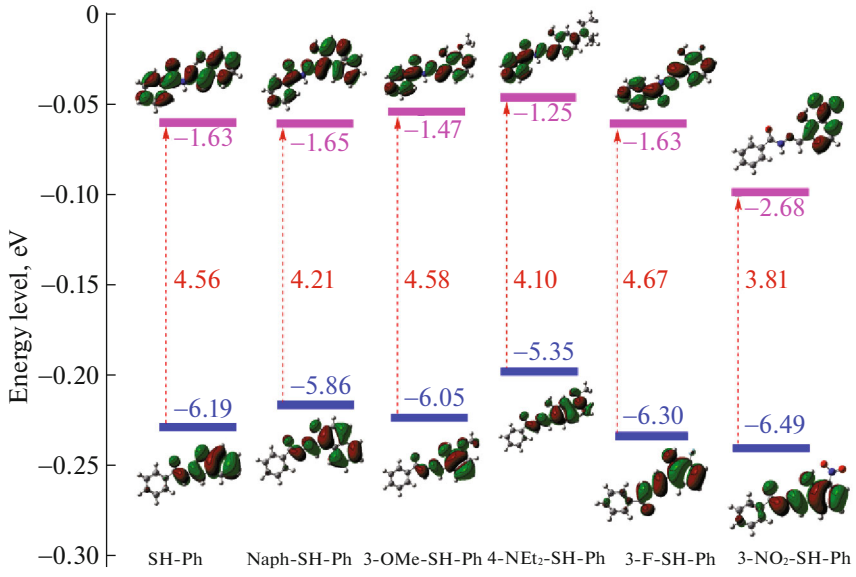

Fig. 4. (Color online) The HOMO and LUMO energies and electronic density contours of the six compounds at S_0 state.

Table 2. Electronic transition data obtained by TD-DFT for the six compounds

Molecule	Electronic transition	E, eV	λ_{cal}, nm	λ_{exp}, nm[a]	f	Main configuration	%
SH-Ph	$S_0 \rightarrow S_1$	3.8406	322.83	325, 296, 284	0.5191	$H \rightarrow L$	96.7
	$S_0 \rightarrow S_2$	4.4661	277.61		0.4625	$H_{-1} \rightarrow L$	87.5
	$S_0 \rightarrow S_4$	4.8664	254.78		0.0890	$H \rightarrow L_{+1}$	91.1
Naph-SH-Ph	$S_0 \rightarrow S_1$	3.5812	346.21	358, 323, 257	0.6279	$H \rightarrow L$	97.8
	$S_0 \rightarrow S_2$	4.2523	291.57		0.1169	$H_{-1} \rightarrow L$	49.9
	$S_0 \rightarrow S_5$	4.7264	262.33		0.1568	$H_{-2} \rightarrow L$	86.6
3-OMe-SH-Ph	$S_0 \rightarrow S_1$	3.8802	319.53	298	0.2997	$H \rightarrow L$	95.3
	$S_0 \rightarrow S_2$	4.2453	292.05		0.7576	$H_{-1} \rightarrow L$	94.4
	$S_0 \rightarrow S_4$	4.8467	255.81		0.0579	$H \rightarrow L_{+1}$	91.7
4-NEt_2-SH-Ph	$S_0 \rightarrow S_1$	3.5574	348.53	366	1.0574	$H \rightarrow L$	98.5
	$S_0 \rightarrow S_2$	4.4200	280.51		0.1792	$H \rightarrow L_{+1}$	54.9
	$S_0 \rightarrow S_3$	4.4715	277.27		0.1732	$H \rightarrow L_{+1}$	42.3
3-F-SH-Ph	$S_0 \rightarrow S_1$	4.0013	309.86	328, 297	0.8426	$H \rightarrow L$	95.5
	$S_0 \rightarrow S_2$	4.3813	282.99		0.2064	$H_{-1} \rightarrow L$	89.3
	$S_0 \rightarrow S_6$	5.2184	237.59		0.0321	$H_{-4} \rightarrow L$	29.6
3-NO_2-SH-Ph	$S_0 \rightarrow S_1$	3.0756	403.12	297	0.1085	$H \rightarrow L$	97.8
	$S_0 \rightarrow S_2$	4.0793	303.94		0.3841	$H_{-2} \rightarrow L$	67.8
	$S_0 \rightarrow S_4$	4.1984	295.31		0.3624	$H_{-1} \rightarrow L$	45.9

[a]The experimental bonds and angle are from [12].

SH-Ph show blue-shift by 12 and 3 nm in the S_1 absorption wavelength, respectively. The S_1 absorption wavelengths of compounds 4-NEt_2-SH-Ph and 3-NO_2-SH-Ph are red-shifted by about 25 and 80 nm relative to compound SH-Ph. Therefore, the diethylamino group as electron-donating and nitro group as electron-withdrawing strongly affects the electronic properties, resulting in a larger increase in S_1 absorption wavelength than fluorine and methoxy groups. As for compound Naph-SH-Ph, the S_1 absorption wavelength is red-shifted compared with compound SH-Ph due to the increasing π-conjugation length.

For all the compounds, the largest absorption wavelengths correspond to different excited states. Different from other compounds, the compounds 3-OMe-SH-Ph and 3-NO_2-SH-Ph have absorption peaks localized at 292.05 and 303.94 nm, which mainly come from the transitions from HOMO-1 → LUMO (94.4%) and HOMO-2 → LUMO (67.8%), respectively. The orbital analysis indicates that the HOMO/HOMO-1 mainly distributed on the salicylaldehyde and imine, and the HOMO-2 is distributed throughout the π-conjugated framework. This can explain the particular absorption peaks of compounds 3-OMe-SH-Ph and 3-NO_2-SH-Ph, and the theoretical absorption spectra agree well with the experimental values [12] with negligible errors.

Emission Spectra

We have calculated the emission spectra of the studied compounds using the optimized geometries of the excited-state at the theoretical level of TD-DFT. The excited state characteristics of the compounds are summarized in Table 3 and the emission peaks with the lowest emission bands are attributed to the electronic transition of $\pi \rightarrow \pi^*$ resulting from the LUMO → HOMO. Neglecting the negligible differences between the calculated and experimental values [12], the calculated results again show the influence of the electron-donating and electron-withdrawing groups with the conjugation of aromatic ring on the properties of fluorescent compounds. Substantially, similar to the absorption spectrum changes, the introduction of fluorine and methoxy group do not significantly change the emission spectrum, whereas the electron-donating diethylamino group and electron-withdrawing nitro group causes red-shift. The large π-conjugated structure also causes red-shift. This is because that the emission peaks with the strongest oscillator strength are mainly attributed to the elec-

Table 3. Emission spectra obtained by TD-DFT method for the six compounds

Molecule	Transition	E, eV	λ_{cal}, nm	λ_{exp}, nm[a]	f	Main configuration	%
SH-Ph	$S_1 \leftarrow S_0$	3.1068	399.07	–	0.8269	H ← L	98.7%
Naph-SH-Ph	$S_1 \leftarrow S_0$	2.8059	441.87	428	0.9768	H ← L	99.1%
3-OMe-SH-Ph	$S_1 \leftarrow S_0$	3.0457	407.07	419	0.8480	H ← L	98.4%
4-NEt_2-SH-Ph	$S_1 \leftarrow S_0$	2.6756	463.39	505	1.0052	H ← L	98.6%
3-F-SH-Ph	$S_1 \leftarrow S_0$	3.1031	399.54	435	1.0953	H ← L	99.1%
3-NO_2-SH-Ph	$S_1 \leftarrow S_0$	2.0604	601.75	435	0.1161	H ← L	99.5%
	$S_2 \leftarrow S_0$	3.4722	357.07		0.6856	H-2 ← L	49.1%

[a]The experimental bonds and angle are from [12].

tronic transition of $\pi \rightarrow \pi^*$ resulting from the LUMO → HOMO. So the HOMO → LUMO gap significantly determined how the emission spectra varied with the substitution and conjugation.

Ionization Potentials and Electron Affinities

A good device performance of OLED is attributed to the good charge mobility and the comparable balance between the holes and electrons [24]. The ionization potentials (*IP*s) and electron affinities (*EA*s) can be used to assess the energy barriers for injecting holes and electrons into compounds, and can be calculated by the DFT on neutral, cation, and anion state geometries. Then, the reorganization energy (λ) is used to approximately estimate the charge transport rate and the balance between hole and electron. The *IP*s and *EA*s were obtained with both vertical (v, at the geometry of the neutral molecule) and adiabatic (a, optimized structures for both the neutral and charged molecules). *HEP* and *EEP* were used to evaluate the extraction potentials for hole and electron, respectively. All these calculated results are given in Table 4. The calculated details are similar as given by [25, 26]. By means of the hopping-type mechanism [27–30] and Marcus theory [31, 32], it is known that the efficient charge transfer is mostly dominated by the value of reorganization energy which can be evaluated by the following relations [25]:

$$\lambda_{hole} = \lambda_0 + \lambda_+ = [E^+(M)] - E^+(M^+)] + [E(M^+) - E(M)] = [E^+(M)] - E(M)] + [E^+(M^+) - E(M^+)] = IP(v) - HEP, \quad (1)$$

$$\lambda_{electron} = \lambda_0 + \lambda_- = [E^-(M)] - E^-(M^-)] + [E(M^-) - E(M)] = [E(M^-)] - E^-(M^-)] + [E(M) - E^-(M)] = EEP - EA(v), \quad (2)$$

where E, E^+, and E represent the energies of the neutral, cation and anion, respectively, and M, M^+, and M represent the geometries of neutral, cation, and anion, respectively. As is known that if the *IP* value is smaller, the hole injection is easier, on the other hand, if the *EA* value is larger, the electron injection is easier. As shown in Table 4, the trends of the *IP*s and *EA*s of the studied compounds are positively the same as HOMO and LUMO energies. The value of $IP(v)$ obey the order of 3-NO_2-SH-Ph > 3-F-SH-Ph > SH-Ph > 3-OMe-SH-Ph > Naph-SH-Ph > 4-NEt_2-SH-Ph, while $EA(v)$ obey the order of 3-NO_2-SH-Ph > Naph-SH-Ph > 3-F-SH-Ph > SH-Ph > 3-OMe-SH-Ph > 4-NEt_2-SH-Ph. Taking compound SH-Ph as a reference, the electron-withdrawing groups (–F and $-NO_2$) can increase the *IP*s and *EA*s, while the electron-donating groups (–OMe and $-NEt_2$) make the *IP*s and *EA*s decrease. The expanded aromatic system (Naph-SH-Ph) can both increase the *EA*s and decrease the *IP*s. These changes show that the ability of Naph-SH-Ph to accept an electron and generate a hole is increasing, which should be conducive to enhancing the injection of electrons and holes in the anode and cathode of light emitting diodes.

There are many factors known to affect reorganization energy (λ), such as heteroatom nature, heterocyclic substituents and conjugation sizes [24]. It has been demonstrated that the larger the $\lambda_{electron}$ and λ_{hole} of the fluorescent material, the weaker the transmission rates of electrons and holes. In Table 3, it is first observed that most λ_{hole} of the six compounds are larger than $\lambda_{electron}$ with the difference varied from 0.04 to 0.18, which means that the hole transport rate is weaker than electron transport the rate. Secondly, we also learn that compared with SH-Ph, the λ_{hole} usually increase by electron-withdrawing groups and decrease by electron-donating groups, while the $\lambda_{electron}$ always increase by electron-withdrawing and electron-donating groups. Furthermore, the strong electron-withdrawing ($-NO_2$) and strong electron-donating groups

Table 4. Ionization potentials (*IP*), electron affnities (*EA*), extraction potentials (*HEP* and *EEP*), and reorganization energies (λ) for each molecule calculated by DFT[a] (eV)

Compound	*IP*(*v*)	*IP*(*a*)	*HEP*	*EA*(*v*)	*EA*(*a*)	*EEP*	λ_{hole}	$\lambda_{electron}$
SH-Ph	6.00	5.80	5.60	1.85	2.01	2.17	0.40	0.32
Naph-SH-Ph	5.64	5.44	5.23	1.87	2.06	2.24	0.41	0.37
3-OMe-SH-Ph	5.86	5.65	5.44	1.69	1.86	2.03	0.42	0.35
4-NEt_2-SH-Ph	5.11	4.94	4.78	1.47	1.69	1.91	0.33	0.44
3-F-SH-Ph	6.12	5.87	5.60	1.85	2.02	2.19	0.52	0.34
3-NO_2-SH-Ph	6.29	6.03	5.76	2.80	3.13	3.47	0.52	0.67

[a]The suffxes (*v*) and (*a*) indicate vertical and adiabatic values, respectively.

(NEt_2) can bring big changes for the values of $\lambda_{electron}$ and λ_{hole} which indicates the introduction of these substituents can improve the charge transfer balance of the compounds, and thus to improve the performance of the OLEDs device. Finally, we have compared and found that the discrepancies between λ_{hole} and $\lambda_{electron}$ in the Naph-SH-Ph and SH-Ph are 0.01 and 0.05 eV, respectively. It concludes that these differences are so small that the expanded aromatic system has very little effect on transmission rates of electrons and holes.

CONCLUSION

Since salicylaldehyde Schiff bases were important typical fluorescent molecules, a comprehensive investigation on six compounds of salicylaldehyde hydrazones (SHs) containing different electron-withdrawing substituent (−F, $-NO_2$) and electron-donating substituents (−OMe, $-NEt_2$) at different position of the aromatic ring has been conducted at the level of PBE1PBE/6-31g(*d,p*) in our work. The calculated geometrical parameters, HOMO, LUMO energies, absorption and emission spectra are well consistent with the reference reports. The calculation results show that different substituents with expanded conjugation of the aromatic system have effect the performance of the optimized geometry, the frontier molecular orbitals, the absorption spectra, the emission spectra and the ionization potentials with electron affinities in different degree. All calculations reveal that introducing strong electron-withdrawing or electron-donating substituents on the base of the expanded aromatic rings is expected to be useful for the luminescent material design.

FUNDING

The work was supported by the Applied Basic Research Programs of Science and Technology Commission Foundation of Chongqing (no. cstc2019jcyj-msxmX0197), Scientific and Technological Research Program of Fuling District Commission (no. FLKJ, 2018BBA3039), Introduction of Yangtze Normal University scientific research grants project (no. 011160011).

REFERENCES

1. B. Valeur, *Molecular Fluorescence: Principles and Applications* (Wiley, Weinheim, Germany, 2002).
2. H. Xiao, K. Chen, D. Cui, N. Jiang, G. Yin, J. Wang, and R. Wang, New J. Chem. **38**, 2386 (2014).
3. M. Gao, C. K. Sim, C. W. T. Leung, Q. Hu, G. Feng, F. Xu, B. Z. Tang, and B. Liu, Chem. Commun. **50**, 8312 (2014).
4. L. Peng, Z. Zhou, R. Wei, K. Li, P. Song, and A. Tong, Dyes Pigments **108**, 24 (2014).
5. J. Mei, N. L. C. Leung, R. T. K. Kwok, J. W. Y. Lam, and B. Z. Tang, Chem. Rev. **115**, 11718 (2015)
6. S. Guieu, F. Cardona, J. Rocha, and A. M. S. Silva, Chem. Eur. J. **65**, 17262 (2018).
7. J. H. Cheng, Y. H. Zhang, X. F. Ma, X. G. Zhou, and H. F. Xiang, Chem. Commun. **49**, 11791 (2013).
8. J. H. Cheng, K. Y. Wei, X. F. Ma, X. G. Zhou, and H. F. Xiang, J. Phys. Chem. C **117**, 16552 (2013).
9. D. Yao, S. Zhao, and J. Guo, J. Mater. Chem. **21**, 3568 (2011).
10. J. Cheng, D. Liu, and W. Li, J. Phys. Chem. C **119**, 4242 (2015).
11. X. F. Ma, J. H. Cheng, J. Y. Liu, X. G. Zhou, and H. F. Xiang, New J. Chem. **39**, 492 (2015).
12. M. Wang, C. Q. Cheng, J. T. Song, J. Wang, X. G. Zhou, H. F. Xiang, and J. Liu, Chin. J. Chem. **36**, 698 (2018).
13. F. L. Zhang and H. S. Huang, Chin. J. Struct. Chem. **10**, 1685 (2017).
14. S. Shahab, L. Filippovich, R. Kumar, M. Darroudi, M. Yousefzadeh Borzehandani, and M. Gomar, J. Mol. Struct. **1101**, 109 (2015).
15. S. Shahab, L. Filippovich, H. A. Almodarresiyeh, M. Sheikhi, and R. Kumar, Chin. J. Struct. Chem. **2**, 186 (2018).
16. S. Shahab, H. Alhosseini Almodarresiyeh, R. Kumar, and M. Darroudi, J. Mol. Struct. **1088**, 105 (2015).
17. S. Masoome, S. Siyamak, F. Liudmila, D. Evgenij, and K. Mehrnoosh, Chin. J. Struct. Chem. **8**, 1201 (2018).

18. E. Runge and E. K. U. Gross, Phys. Rev. Lett. **52**, 997 (1984).
19. M. J. Frisch, G. W. Trucks, H. B. Schlegel, G. E. Scuseria, M. A. Robb, J. R. Cheeseman, G. Scalmani, V. Barone, B. Mennucci, G. A. Petersson, H. Nakatsuji, M. Caricato, X. Li, H. P. Hratchian, A. F. Izmaylov, et al., *Gaussian 09* (Gaussian, Inc., Wallingford, CT, 2009).
20. H. L. Wang, H. Zou, and Y. J. Hu, Chin. J. Struct. Chem. **30**, 1656 (2011).
21. M. Sheikhi, D. Sheikh, and A. Ramazani, S. Afr. J. Chem. **67**, 151 (2014).
22. A. Frisch, A. B. Nielsen, and A. J. Holder, *Gauss View Users Manual* (Gaussian Inc., 2008).
23. H. Uoyama, K. Goushi, K. Shizu, H. Nomura, and C. Adachi, Nature (London, U.K.) **492**, 234 (2012).
24. J. F. Wang, H. Y. Ning, L. Yang, and J. X. Zhang, Opt. Mater. **84**, 694 (2018).
25. B. C. Lin, C. P. Cheng, and Z. P. M. Lao, J. Phys. Chem. A **107**, 5241 (2003).
26. A. Curioni, M. Boero, and W. Andreoni, Chem. Phys. Lett. **294**, 263 (1998).
27. G. R. Hutchison, M. A. Ratner, and T. J. Marks, J. Am. Chem. Soc. **127**, 2339 (2005).
28. A. J. Epstein, W. P. Lee, and V. N. Prigodin, Synth. Met. **117**, 9 (2001).
29. J. A. Reedijk, H. C. F. Marks, S. M. C. van Bohemen, O. Hilt, H. B. Brom, and M. A. Michels, J. Synth. Met. **101**, 475 (1999).
30. N. F. Mott and E. A. Davis, *Electronic Processes in Non-Crystalline Materials,* 2nd ed. (Oxford Univ. Press, Oxford, 1979).
31. R. A. Marcus, Rev. Mod. Phys. **65**, 599 (1993).
32. R. A. H. Marcus and A. Eyring, Rev. Phys. Chem. **15**, 155 (1964).